Environmental Technology & Innovation 21 (2021) 101218

Contents lists available at ScienceDirect

Environmental Technology & Innovation

journal homepage: www.elsevier.com/locate/eti

Synergistic interaction and biochar improvement over co-torrefaction of intermediate waste epoxy resins and fir

Chia-Yang Chen [a], Wei-Hsin Chen [a,b,c,*], Steven Lim [d,e], Hwai Chyuan Ong [f], Aristotle T. Ubando [g]

[a] Department of Aeronautics and Astronautics, National Cheng Kung University, Tainan 701, Taiwan
[b] Research Center for Smart Sustainable Circular Economy, Tunghai University, Taichung 407, Taiwan
[c] Department of Mechanical Engineering, National Chin-Yi University of Technology, Taichung 411, Taiwan
[d] Department of Chemical Engineering, Lee Kong Chian Faculty of Engineering and Science, Universiti Tunku Abdul Rahman, 43000 Kajang, Selangor, Malaysia
[e] Centre for Photonics and Advanced Materials Research, Universiti Tunku Abdul Rahman, 43000 Kajang, Selangor, Malaysia
[f] School of Information, Systems and Modelling, Faculty of Engineering and Information Technology, University of Technology Sydney, NSW 2007, Australia
[g] Mechanical Engineering Department, De La Salle University, 2401 Taft Avenue, Manila 0922, The Philippines

ARTICLE INFO

Article history:
Received 17 July 2020
Received in revised form 28 September 2020
Accepted 26 October 2020
Available online 31 October 2020

Keywords:
Intermediate waste epoxy resins
Fir
Torrefaction and co-torrefaction
Synergistic and antagonistic effects
Blocking effect
Tar

ABSTRACT

This study investigated the synergistic effect of co-torrefaction with intermediate waste epoxy resins and fir in a batch-type reactor towards biochar improvement. The synergistic effect ratio was used to judge the interaction between the two materials assisted by statistical tools. The main interaction between the feedstocks was the catalytic reaction and blocking effect. Sodium presented in the intermediate waste had a pronounced catalytic effect on the liquid products during torrefaction. It successfully enhanced the volatile matter emissions and exhibited an antagonistic effect on the solid yield. Different from the catalytic reaction that occurred during short retention time, the blocking effect was more noticeable with a longer duration, showing a synergistic effect on the solid yield. Alternatively, a significantly antagonistic effect was exerted on oxygen content, while the carbon content displayed a converse trend. This gave rise to a major antagonistic effect on the O/C ratio which was closer to coal for pure materials torrefaction. The other spotlight in this study was to reuse the tar as a heating value additive. After coating it onto the biochar, the higher heating value could be increased by up to 5.4%. Although tar is considered as an unwanted byproduct of torrefaction treatment, the presented data show its high potential to be recycled into useful calorific value enhancer. It also fulfills the scope of waste-to-energy in this study.

1. Introduction

The space for the landfill in Taiwan is going to be saturated in the near future. Even though incineration can reduce a large volume of waste (Chang et al., 1998; Yang et al., 2012), the landfill is still needed for the incombustible matters. Consequently, a more sustainable and economical waste management strategy needs to be devised in Taiwan and worldwide (Ge et al., 2020; Lam et al., 2019). However, there is another important issue in Taiwan currently. Due to

* Corresponding author at: Department of Aeronautics and Astronautics, National Cheng Kung University, Tainan 701, Taiwan.
E-mail addresses: weihsinchen@gmail.com, chenwh@mail.ncku.edu.tw (W.-H. Chen).

https://doi.org/10.1016/j.eti.2020.101218
2352-1864/

the natural limitation, Taiwan heavily relies on external imports for energy sources (∼98%) (Yang et al., 2018). This may create energy security problems (Yao et al., 2018) since the basic element, energy, is dependent on third parties. As a result, developing a self-reliant energy source is a priority. Combining the above two important issues, waste-to-energy is a promising method as it mitigates not only the waste problem but also satisfies the demand for energy at the same time (Chen et al., 2017a).

Among all the wastes, the amount of electronic waste (e-waste) is believed to keep increasing worldwide in the future (Cui and Forssberg, 2003; Zhao et al., 2017). Furthermore, it has a high possibility of causing irreversible damages to the environment (Cui et al., 2017) and human beings (Huang et al., 2016; Labunska et al., 2015) if it does not being treated properly. Among e-wastes, the waste epoxy resin occupies a very high proportion as it is the main component of printed circulated boards (PCBs) (Chikhi et al., 2002) which exists in all the e-wastes. Therefore, transforming waste epoxy resin into energy should be the main priority in waste-to-energy scope and that can display a great influence.

Torrefaction is a favorable thermal pretreatment that is capable of condensing the energy density of biomass (Chen et al., 2015a; Keivani et al., 2018; Kutlu and Kocar, 2018). For instance, under the torrefaction temperature of 260 °C with an hour duration, the HHV was enhanced by 15.3, 16.9, and 6.3% for wheat straw, rice straw, and cotton gin waste, respectively (Sadaka and Negi, 2009). The 6%–18% increment of HHV was also obtained by yellow poplar after torrefaction treatment found by Kim et al. (2012). Moreover, the torrefied biomass possesses the merits of hydrophobic (Chen et al., 2015c; Pimchuai et al., 2010), non-biodegradable (van der Stelt et al., 2011), and high grindability (Correia et al., 2017; Gil et al., 2015) which are conducive to industrial applications. Consequently, transforming waste epoxy resin into energy by using torrefaction might be a beneficial method. Besides, it is well-known that the quality of waste can vary greatly, depending on the sources. It is difficult to control the operating parameters if the properties of the fuel are dissimilar. Whereupon, the traditional biomass–fir was mixed with the waste epoxy resin to perform co-torrefaction in this study, and it is hypothesized that the quality of fuel products will be alike after mixing (Chen and Chen, 2020). In addition to soothing the unstable quality of wastes, blending with fir can greatly reduce air pollutant emissions if biochar is used as a fuel for combustion (Chen et al., 2021). That is attributed to the higher oxygen content in the biofuel (Chen et al., 2017a; Cheruiyot et al., 2019), which will create more complete combustion (Chen et al., 2017b; Tsai et al., 2015).

Several previous studies had focused on the co-thermal treatment such as co-pyrolysis between waste resins and traditional biomass and their interaction effects. For example, the synergistic effect on the liquid and gas yields were discovered after biomass was blended with plastic materials (Sajdak, 2017). A similar result was also found by Brebu et al. (2010). After pine cone was added into the synthetic polymers, more gas-phase products were presented than the theoretical value associated with lower char yield. On the other hand, Wu and Qiu (2014) announced that the antagonistic phenomenon was discovered in the total volatile matters (liquid + gas) in the case of co-pyrolysis between Chinese fir and printed circuit boards (PCBs) waste.

From the prior literature, most of the studies merely referred to the synergistic or antagonistic effect on the product yields. Further investigations about the interaction impact on basic proximate analysis, elemental analysis, and high heating value (HHV) of the product are still lacking. In this study, a batch type reactor was used to conduct the co-torrefaction of epoxy resin and fir. The sample amount was sufficient to conduct the proximate analysis, elemental analysis, and HHV so that the interaction on the aforementioned analyses could be well-explained. The other highlight in this study is the usage of tar, an unwanted waste produced from torrefaction, as an HHV enhancer. Based on the data elaborated in this study, it can solve the intermediate waste epoxy resin problems without tar issue, accomplishing the vision of waste-to-energy conversion.

2. Experimental

2.1. Materials

Two intermediate waste epoxy resins (WE1 and WE2) were collected from two different processes. WE1 was from the production of phenolic epoxy, while the liquid-type epoxy resin manufacture process was the source for WE2. A biomass material, fir, was chosen to blend with waste epoxy resins which were provided by CPC Corporation, Taiwan.

All the materials were subjected to the same pretreatments to provide an identical basis. After putting the feedstocks in a shredder, they were collected with the size under 0.149 mm (passing 100 mesh). Prior to experiments, both fir and waste epoxy resins were stored in the oven (50 °C) for at least 24 h. The co-torrefaction experiments were conducted at fir-to-waste epoxy resin mixing ratios of 1:0, 3:1, 1:1, 1:3, and 0:1 on a weight basis. After weighting waste epoxy resins and fir individually, both of them were put in the same glass tubes with caps. Then, vigorously shaken was conducted to mix the waste epoxy resin and fir evenly before the reaction. The even quality was tested by the concentric sampling method, and the maximum difference was not greater than 1.3%.

2.2. Batch type reactor system and experimental procedure

The schematic diagram of the batch type reactor system is shown in Fig. 1. The whole system could be partitioned into three parts: inlet, main body, and outlet. The inlet part consisted of a gas cylinder full of nitrogen (Purity > 99%) and a flow meter. The flow rate of nitrogen was set as 100 mL/min. The main body part of this system included a glass tube,

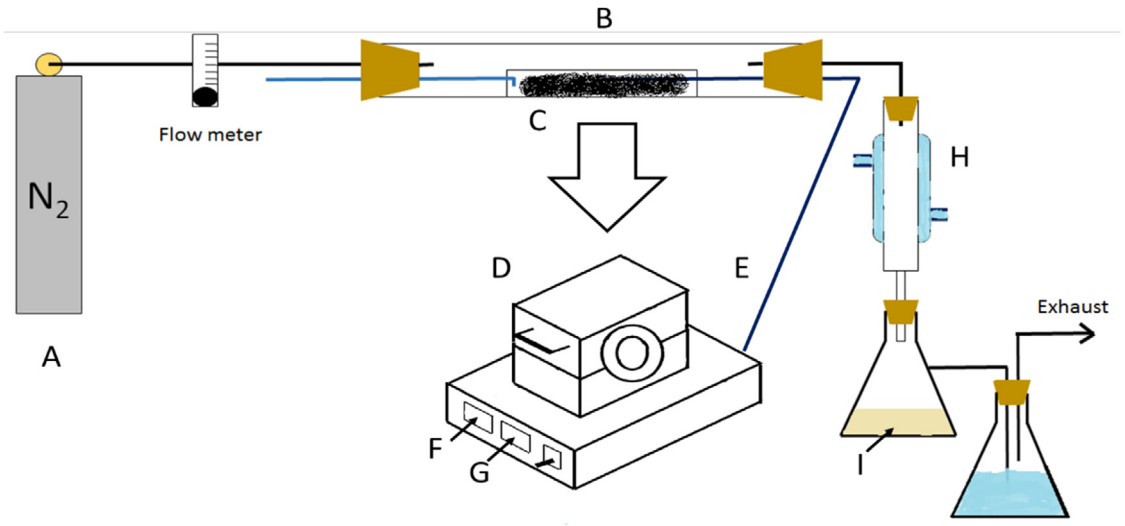

Fig. 1. The schematic of the conducted torrefaction experiment. (A=gas cylinder, B=glass tube, C=boat with feedstock/biochar, D=furnace, E=thermocouple, F=temperature controller for furnace, G=temperature monitor of thermocouple, H=cooler, and I= bio-oil).

a boat, a hook, and a furnace with a K-type thermocouple. The boat loaded materials for the torrefaction reaction. The weight of the tested materials was around 30 g in each run. After supplying a tested material, the boat was put inside of the glass tube and the glass tube was sealed by two plugs. A hook was inserted into the plug to control the location of the boat. Thereafter, the glass tube with a boat was placed in the furnace and the thermocouple was fixed at the center of the sample pile. The temperature of the furnace was controlled at 300 °C which pertained to the severe torrefaction (Chen and Chen, 2020). The temperature of the tested sample was displayed on the monitor through the thermocouple. When the temperature of the tested sample achieved 300 °C, the duration time started to count. Three duration times including 20 min, 40 min, and 60 min were considered in this study. After finishing the torrefaction treatment, the boat with torrefied biomass (char) was pulled out of the glass tube by the hook. The weight percentage of char to the raw biomass was measured for the solid yield.

The outlet part of this system comprised a cooling system and two cylinders. The cooling system was a straight glass tube with a water coat. The water coat was filled with ice water (4 °C) which was supplied by a cooling water cycler. After passing the cooling system, the condensable matters were collected by the first cylinder and they represented the liquid product of torrefaction. The liquid yield was calculated to be the weight ratio of the liquid product to the original weight, while the gas yield was calculated by mass balance. The next cylinder contained water and the connecting pipe was inserted under the water level. This was used to check the leakage of the system. If the system was sealed well, nitrogen could arrive at the last cylinder and there were a lot of bubbles during the experiments. Prior to experiments, the flow rate conservation was also ascertained by measuring the nitrogen flow rate at the exit.

2.3. Analysis of torrefied biomass

After getting the torrefied products from the batch type reactor, several analyses including proximate analysis, elemental analysis, and high heating value (HHV) were tested. The same basis conditions (50 °C and 100 mesh) for torrefaction experiments were also set before the proximate analysis for comparison. The proximate analysis was performed based on the standard procedure of ASTM E870-82. The moisture content of a sample was the ratio of the weight difference before and after the drying process at 105 °C for 1 h. The remaining weight of a sample after heating in a furnace at 590 °C for 3 h represents its ash content. Volatile matter (VM) was evaluated by the weight reduction under 950 °C heating without oxygen for 7 min. The fixed carbon (FC) content was calculated by mass balance, that is, FC = 100 - moisture - ash - VM.

Before conducting the elemental analysis and HHV, all of the materials were dried in an oven at 105 °C for at least 12 h to set the dry basis. After that, the elemental contents including C, H, N, and S were analyzed by an elemental analyzer (PerkinElmer 2400 Series II CHNS/O Elemental Analyzer). The O content was attained by mass balance (i.e., $O = 100 - C - H - N - S$), while the HHVs of the samples were measured by a bomb calorimeter (IKA C6000).

To characterize the chemical composition of the torrefied biomass, a Fourier transform infrared (FTIR) spectrometer (Perkin Elmer Spectrum 100) coupled with the attenuated total reflectance (ATR) was used to target the specific chemical bondings where the wavenumber range was between 600 and 4000 cm^{-1}. According to the feedstock and products of waste epoxy resin, several compounds with specific wavenumbers were identified and listed in **Table S1**. To ensure

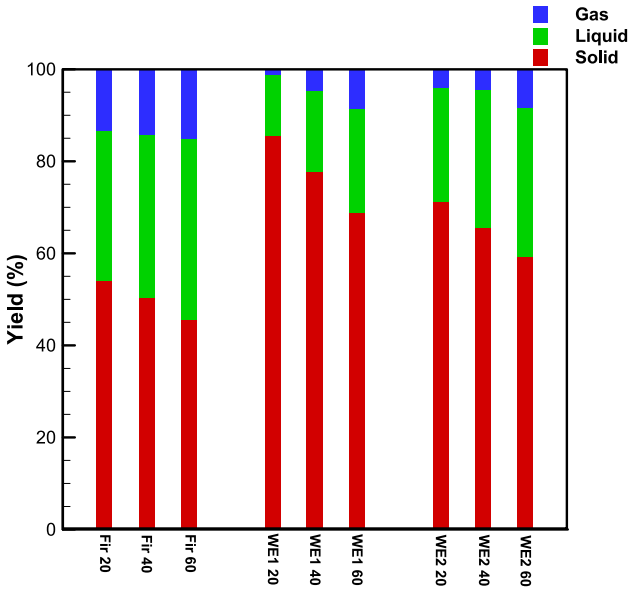

Fig. 2. The gas, liquid, and solid yields of pure materials with three different torrefaction retention times.

the reliability of the experiments, several samples were randomly picked to perform duplicate tests. The duplicate tests included the torrefaction experiments for mass yield, HHV tests, proximate analysis, and elemental analysis. The maximum difference among these duplicate tests was lower than 3%.

3. Results and discussion

3.1. Product yields after torrefaction

3.1.1. Individual materials

The solid, liquid, and gas yields of the three individual materials (i.e., fir, WE1, and WE2) were shown in Fig. 2. It could be discovered that the solid yields for WE1 and WE2 were higher than fir, independent of the retention time. On the contrary, the liquid and gas yields from fir were higher than the intermediate epoxy resins (WE1 and WE2), as a consequence of the higher thermal resistance of epoxy resins than fir (Chen et al., 2020a). Consequently, the thermal treatment showed less influence on the waste epoxy resins, especially in producing liquid and gaseous products.

With increasing the torrefaction duration, the solid yield gradually decreased coupled with the increasing the liquid and gas yields regardless of feedstock. It was attributed to the materials experiencing thermal energy for a longer period and more torrefaction reaction was exerted on the materials. For the duration increased from 20 to 60 min, the solid yield reduced from 54% to 45%, 85% to 68%, and 71% to 59% for fir, WE1, and WE2, respectively. A similar study in the literature also showed that the solid yield would decrease with longer holding time (Bach et al., 2017). Fig. 2 depicted that the effect of retention time was more pronounced on WE1 although it showed the highest thermal resistance on the average solid yield. The possible reason was that a longer duration was necessary for high thermal resistance material like WE1 to react, while fir required a shorter time to complete the whole reaction.

3.1.2. Mixtures

The theoretical value, experimental value, and synergistic effect were listed in Table 1. The theoretical number was calculated by the summation of the two materials with the specific mixing ratio under the specific retention time. For instance, the theoretical value for the solid yield of Fir: WE1 1:1 with 20 min duration was calculated using the following equation (Lu et al., 2013):

$$\text{Theoretical value} = \textit{solid yield}_{Fir20} \times 0.5 + \textit{solid yield}_{WE20} \times 0.5 \quad (1)$$

Meanwhile, the synergistic effect (SE) was calculated according to the difference between theoretical and experimental value:

$$\text{SE} = \frac{\text{experimental} - \text{theoretical}}{\text{theoretical}} \times 100 \quad (2)$$

Most of the mixture of fir and WE1 showed an antagonistic effect (negative value) in the solid yield, while the SE for liquid yield for the same mixture showed a reverse trend in which most of them were positive values. On the other hand,

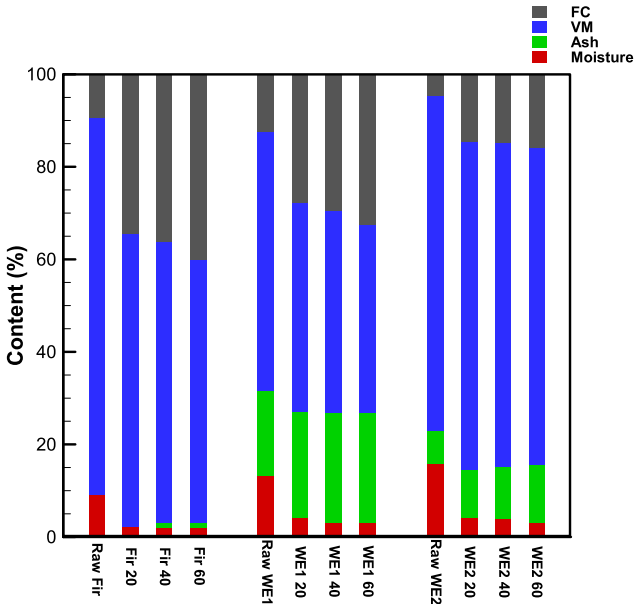

Fig. 3. The proximate analysis of pure materials with three different torrefaction retention times.

Table 1
The synergistic effect (SE) on product yields of the tested mixtures after torrefaction with different retention times.

Mixtures	Solid yield (%)			Liquid yield (%)			Gas yield (%)		
	Theo.	Exp.	SE (%)	Theo.	Exp.	SE (%)	Theo.	Exp.	SE (%)
Fir: WE1 (duration)									
3:1 (20)	61.72	60.07	−3.02	28.25	29.55	4.60	10.03	10.38	3.49
3:1 (40)	57.13	56.30	−1.45	31.50	32.62	3.56	11.37	11.07	−2.64
3:1 (60)	50.41	50.64	−1.27	35.83	35.18	−1.81	13.75	14.18	3.13
1:1 (20)	69.77	63.28	−9.31	22.90	27.34	19.39	7.33	9.38	27.99
1:1 (40)	63.98	59.71	−6.67	26.48	30.10	13.67	9.54	10.19	6.80
1:1 (60)	57.13	57.05	−0.12	30.98	31.82	2.71	11.89	11.12	−6.48
1:3 (20)	77.60	76.86	−0.96	18.08	18.07	−0.06	4.32	5.07	17.56
1:3 (40)	70.83	72.08	1.77	22.01	22.07	0.27	7.16	5.84	−18.36
1:3 (60)	62.96	64.77	2.87	26.81	24.79	−7.53	10.23	10.44	2.07
Fir: WE2(duration)									
3:1 (20)	58.38	54.12	−7.30	30.60	31.52	3.01	11.02	14.36	30.31
3:1 (40)	54.08	51.09	−5.53	34.08	32.19	−5.55	11.84	16.72	41.27
3:1 (60)	48.92	50.21	2.64	37.56	34.03	−9.39	13.52	15.76	16.55
1:1 (20)	62.66	60.68	−3.15	28.65	25.28	−11.78	8.69	14.04	61.56
1:1 (40)	57.87	58.78	1.58	32.75	29.44	−10.13	9.38	11.78	25.65
1:1 (60)	52.38	55.12	5.24	35.79	31.25	−12.68	11.83	13.63	15.17
1:3 (20)	66.93	64.05	−4.30	26.71	29.01	8.60	6.36	6.94	9.11
1:3 (40)	61.67	62.64	1.58	31.42	30.50	−2.94	6.91	6.86	−0.75
1:3 (60)	55.84	59.20	6.02	34.02	33.07	−2.78	10.14	7.73	−23.80

the SE for the mixtures of fir and WE2 displayed more positive values in the solid yield compared to those of fir and WE1; the SE for the liquid yield also showed an inverse trend to the fir and WE1 counterparts. As for the duration, the mixtures of fir and WE1 as well as fir and WE2 showed a similar trend where the SE value gradually increased with increasing duration. Accordingly, it was summarized that a shorter duration (20 min) resulted in a more antagonistic effect, whereas a longer one (60 min) led to a more synergistic effect.

There were two important interaction reactions between fir and intermediate waste epoxy resins. One was the catalytic effect and the other the blocking effect. The former was due to the presence of sodium chloride in the intermediate wastes. It was one of the catalysts used in the production process of epoxy resins. Sodium is well-known for its catalytic ability in increasing liquid products after torrefaction (Khazraie Shoulaifar et al., 2016; Mazaheri et al., 2013). Consequently, even though the retention time was short, the sodium was still able to accelerate the reaction rate. This resulted in an increase in volatile matter emission with lower solid yield, as shown in Table 1. Nevertheless, the catalyst could only accelerate the reaction rate without affecting the original reaction pathway. If the retention time increased, the reaction would become more complete and mitigate the antagonistic effect (catalytic effect).

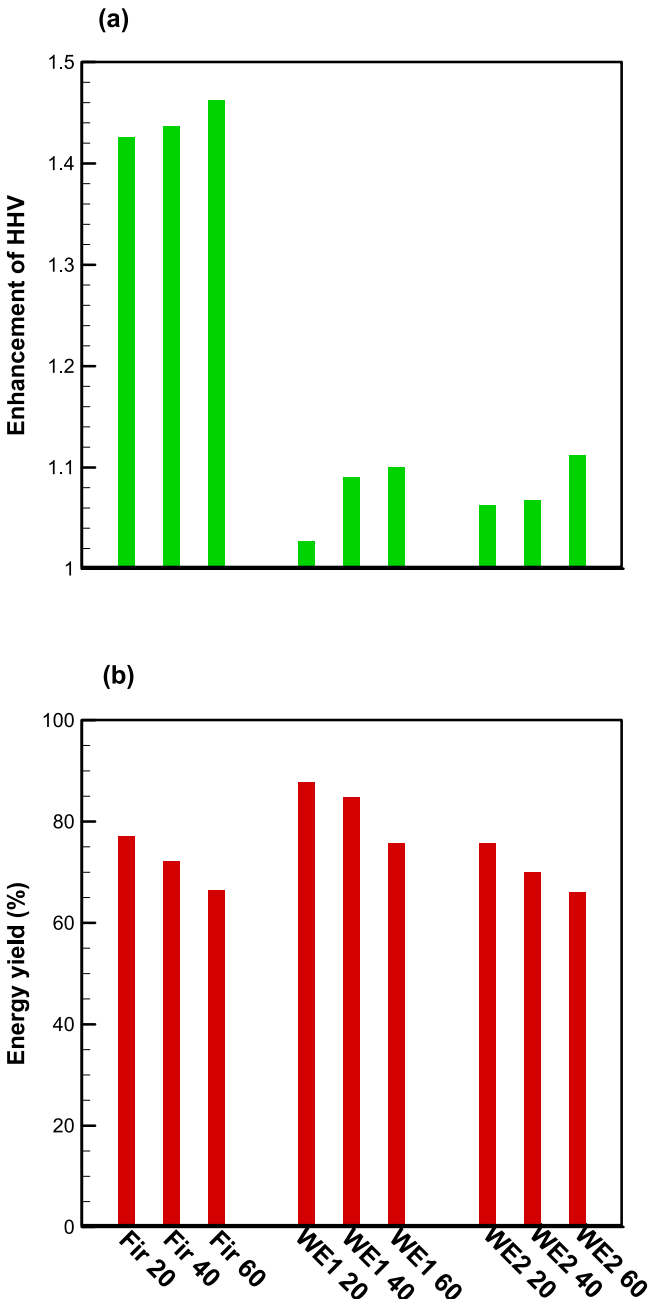

Fig. 4. The (a) enhancement of HHV and (b) energy yield of the biochars from three pure materials after torrefaction treatment.

Thereafter, the other interaction between fir and waste epoxy resin, namely, the blocking effect, became more dominant. The blocking effect from the inert material would block the active sites of volatile matter emission and subsequently increase the solid yield (Darmstadt et al., 2001). That could explain the discovery of a more synergistic effect in the solid yield of the mixture of fir and WE2. It stemmed from the density difference between WE1 and WE2. WE2 had a much lower density compared to WE1. For the same weight ratio, the volume of WE2 was around double of WE1. As a result, the blocking effect was more pronounced for WE2 compared to WE1.

Table 2
The synergistic effect (SE) on proximate analysis of the tested mixtures biochar after torrefaction with different retention times.

Mixtures	Moisture	Ash	VM			FC		
	Exp.	Exp.	Theo.	Exp.	SE (%)	Theo.	Exp.	SE (%)
Fir: WE1 (duration)								
3:1 (20)	3.06	5.94	58.83	56.55	−3.88	32.95	32.47	−1.47
3:1 (40)	1.98	8.16	56.55	55.14	−2.49	34.58	33.70	−2.56
3:1 (60)	1.92	10.38	52.83	51.87	−1.82	38.28	35.83	−6.40
1:1 (20)	3.00	15.09	54.30	52.23	−3.81	31.25	31.56	0.99
1:1 (40)	2.04	18.09	52.28	50.79	−2.85	32.91	31.21	−5.17
1:1 (60)	1.92	19.61	48.74	48.08	−1.36	36.40	32.35	−11.13
1:3 (20)	3.92	17.14	49.76	49.82	0.11	29.55	29.12	−1.47
1:3 (40)	2.91	19.59	48.02	48.03	0.02	31.23	29.47	−5.66
1:3 (60)	2.11	20.59	44.65	45.25	1.34	34.52	32.05	−7.16
Fir: WE2 (duration)								
3:1 (20)	2.91	4.00	65.27	64.06	−1.86	29.67	29.03	−2.17
3:1 (40)	2.70	3.77	63.09	61.92	−1.86	30.95	31.61	2.11
3:1 (60)	2.00	4.04	59.81	59.19	−1.04	34.12	34.77	1.90
1:1 (20)	3.64	5.00	67.17	66.86	−0.46	24.69	24.50	−0.79
1:1 (40)	2.75	5.77	65.37	65.16	−0.33	25.65	26.32	2.64
1:1 (60)	2.06	6.38	62.70	63.16	0.72	28.08	28.40	1.13
1:3 (20)	3.96	6.93	69.08	68.46	−0.89	19.71	19.37	−1.74
1:3 (40)	2.88	7.34	67.66	68.27	0.90	20.34	20.59	1.22
1:3 (60)	1.87	7.69	65.60	66.28	1.04	22.04	23.20	5.23

3.2. Proximate analysis

3.2.1. Individual materials

Fig. 3 depicted that, for all the materials, the moisture content was clearly diminished after torrefaction treatment, attributing to torrefied biomass becoming more hydrophobic (Chen et al., 2018). The ash content magnified after torrefaction because of the deduction of the total weight of biomass, whereas the FC content increased ascribing to the reduced VM content. A similar result was also reported by a previous paper (Lu and Chen, 2013). The carbonization level was in the order of Fir > WE2 > WE1 after torrefaction in that the FC content increased by the factors of 288%, 218%, and 139% for Fir, WE2, and WE1, respectively. The dominant molecular structure of WE1 was cross-linked aromatic rings, while WE2 was a long straight chain structure. Although both of them contained aromatic rings, a higher cross-linked structure usually exhibited higher thermal resistance (Sher et al., 2020).

For the effect of duration, it was only statistically significant on the FC and VM but not for moisture and ash content. Based on the data shown in Fig. 3, the p-values of FC and VM were calculated to be lower than 0.05, whereas the p-values of the moisture and ash contents were higher than 0.05, investigated by t-test at $\alpha = 0.05$. Consequently, the duration did play a significant role in increasing the FC content inside of biochar, although the increment was not very huge (Sadaka and Negi, 2009). On the contrary, the VM content declined with a longer duration. When more VM content was liberated away due to longer retention time, the solid yield dropped correspondingly (Fig. 2) (Babinszki et al., 2020).

3.2.2. Mixtures

The theoretical and experimental values of proximate analysis were tabulated in Table 2 in which the SE values of VM and FC were calculated. The inert property for moisture and ash contents should have negligible interaction in this reaction, so their SE values were not determined. From the ANOVA test, the influence of duration and mixing ratio on the VM and FC contents were proven to be significant (both p-value < 0.05). It was discovered that most of the VM content in the fir and WE1 mixture presented an antagonistic effect. That implied more VM was liberated during torrefaction than the theoretical values, which might be assigned to the effect of catalyst.

The antagonistic effect on the VM content decreased and even became a synergistic effect when the duration was enlarged. This was consistent with the previous explanation. The catalytic effect would be mitigated when the reaction progressed to the end-stage. At this moment, the other interaction effect (blocking effect) would become more dominant. When the mixing proportion of waste epoxy resins was increased, the blocking effect was more prominent. The mixing ratio of 1:3 presented a more pronounced synergistic effect on VM content, as shown in Table 2. The trend of FC was inversely proportional to the trend of VM. That is, if the VM content decreased, the FC content magnified, and vice versa.

3.3. Enhancement of HHV and energy yield

3.3.1. Individual materials

The enhancement in HHV after torrefaction for the individual materials are shown in Fig. 4a. It clearly displayed that the torrefaction effect was more drastic on fir compared to waste epoxy resins. During torrefaction, the majority of the hemicelluloses would be destroyed and liberated away from biomass (Ong et al., 2020), whereas the remained cellulose

Table 3
The synergistic effect (SE) on energy yields of the tested mixtures after 20-min torrefaction with different mixing ratios.

Mixtures	Solid yield (%)			Enhancement of HHV			Energy yield (%)		
	Theo.	Exp.	SE (%)	Theo.	Exp.	SE (%)	Theo.	Exp.	SE (%)
Fir:WE1 3:1	61.94	60.07	−3.02	1.31	1.32	0.48	81.27	79.20	−2.55
Fir:WE1 1:1	69.77	63.28	−9.31	1.21	1.24	2.33	84.34	78.27	−7.20
Fir:WE1 1:3	77.60	76.86	−0.96	1.11	1.12	0.21	86.44	85.79	−0.75
Fir:WE2 3:1	58.38	54.12	−7.30	1.31	1.31	−0.21	76.76	71.01	−7.49
Fir:WE2 1:1	62.66	60.68	−3.15	1.22	1.22	0.07	76.40	74.04	−3.09
Fir:WE2 1:3	66.93	64.05	−4.30	1.14	1.13	−0.17	76.04	72.65	−4.46

and lignin would pose higher HHVs in the torrefied biomass., rendering an increase in the energy density of the biofuel after torrefaction (Chen et al., 2015c). On the other hand, the higher heat resistance property of epoxy resin inhibited the influence of torrefaction (Chen et al., 2020a). The main gap in HHV enhancement is between 20 and 40 min for WE1, while it is between 40 and 60 min for WE2. The possible reason is that the VM content in WE1 has lower thermal resistance than the one in WE2. Consequently, the VM in WE1 can liberate within a shorter retention time (40 min), rendering the carbonization effect. On the contrary, the VM in WE2 with greater thermal resistance requires a longer retention time (60 min) to achieve carbonization. The impact of duration on intensifying HHV was more conspicuous for waste epoxy resins compared to fir. The enhancement of HHV increased by about 3% for fir, while for waste epoxy resins, the enhancement was almost doubled for duration increased from 20 to 60 min.

The energy yield was calculated by multiplying the solid yield and the enhancement of HHV (Chen et al., 2014). For the energy yields of three materials (Fig. 4b), fir and WE2 were similar (around 70%) while the average energy yield for WE1 was more than 80%. With increasing duration, the energy yield decreased and similar results were reported in a previous study (Bach et al., 2017). This implied, in turn, that the enhancement of HHV was not able to compensate for the higher loss of the solid yield in the feedstock. Consequently, the following results on the mixtures with different blending ratios would be tested only for 20 min duration due to the highest energy yield.

3.3.2. Mixtures

The SE on the enhancement of HHV and energy yields for the mixtures with different blending ratios were listed in Table 3. Most of the SE were either antagonistic or slightly higher than zero, while the highest synergistic value was 2.33%. Based on the mixing ratio effect, the blending ratio of 1:1 would allow fir to react with waste epoxy resin in an equal chance, whereas the other blending ratios were not balanced. As a result, the mixing ratio of 1:1 might trigger more interaction between fir and waste epoxy resin that led to the higher SE value. That is, the synergistic/antagonistic performance was different between 1:1 and 3:1 or 1:3. Similar results were also obtained by Wu and Qiu (2014). They reported that co-pyrolysis between fir and waste PCBs would produce more brominated aromatic compounds at the blending ratios 1:4 (14.84 wt%) and 4:1 (10.96 wt%) compared to 1:1 (7.98 wt%). The brominated aromatic compounds were well-known as a flame retardant (John Kennedy et al., 2015). The corresponding SE for the FC content was also in the same trend. For 20 min duration, the SE of the FC content at Fir: WE1 = 1:1 was 0.99, whereas the other two mixing ratios demonstrated negative values. The same observation also applied to the case between Fir and WE2 where the SE of the blending ratio of 1:1 had the highest value among all the three mixing ratios.

However, for the mixture between fir and WE1, the SE of the energy yield for at 1: 1 blending ratio was the lowest. This was due to the higher antagonistic effect exerted on the solid yield at the ratio. The synergistic effect of the enhancement of HHV allowed the corresponding solid yield to decrease (VM vaporization), so the energy density was condensed (Chen et al., 2015c). On the contrary, for the mixtures of fir and WE2, the SE presented the highest values in both the solid yield and the enhancement of HHV at 1:1 mixing ratio. This was primarily attributed to the contents inside WE2 which possessed higher HHV. Consequently, the higher solid loss also resulted in HHV decline. The HHV of WE2 (23.6 MJ/kg) was higher than that of WE1 (21.3 MJ/kg). The variation of SE for the enhancement of HHV was almost similar to the solid yield, as evidenced by this point. Compared to the enhancement of HHV, the solid yield exhibited a larger change by approximately one order of magnitude. Therefore, from the data of the energy yield, the synergistic effect on the enhancement of HHV was less significant compared to the antagonistic effect on the solid yield; which means, the energy yield of the products would be highly dependent on the corresponding solid yield.

3.4. Elemental analysis

3.4.1. Individual materials

Fig. 5 demonstrated that the carbon content increased with the reduction of the other elements after torrefaction, regardless of materials, due to the carbonization effect. Past studies have also illustrated the same tendency (Chen et al., 2012). As described earlier, the carbonization effect on the feedstock was in the order of Fir > WE2 > WE1. The increment of carbon content was around 29% for fir, 7.7% for WE2, and 4.0% for WE1. Since carbon is the main source of heat energy of biofuels, the corresponding enhancement of HHV also presented a similar trend. Consequently, although raw fir has the

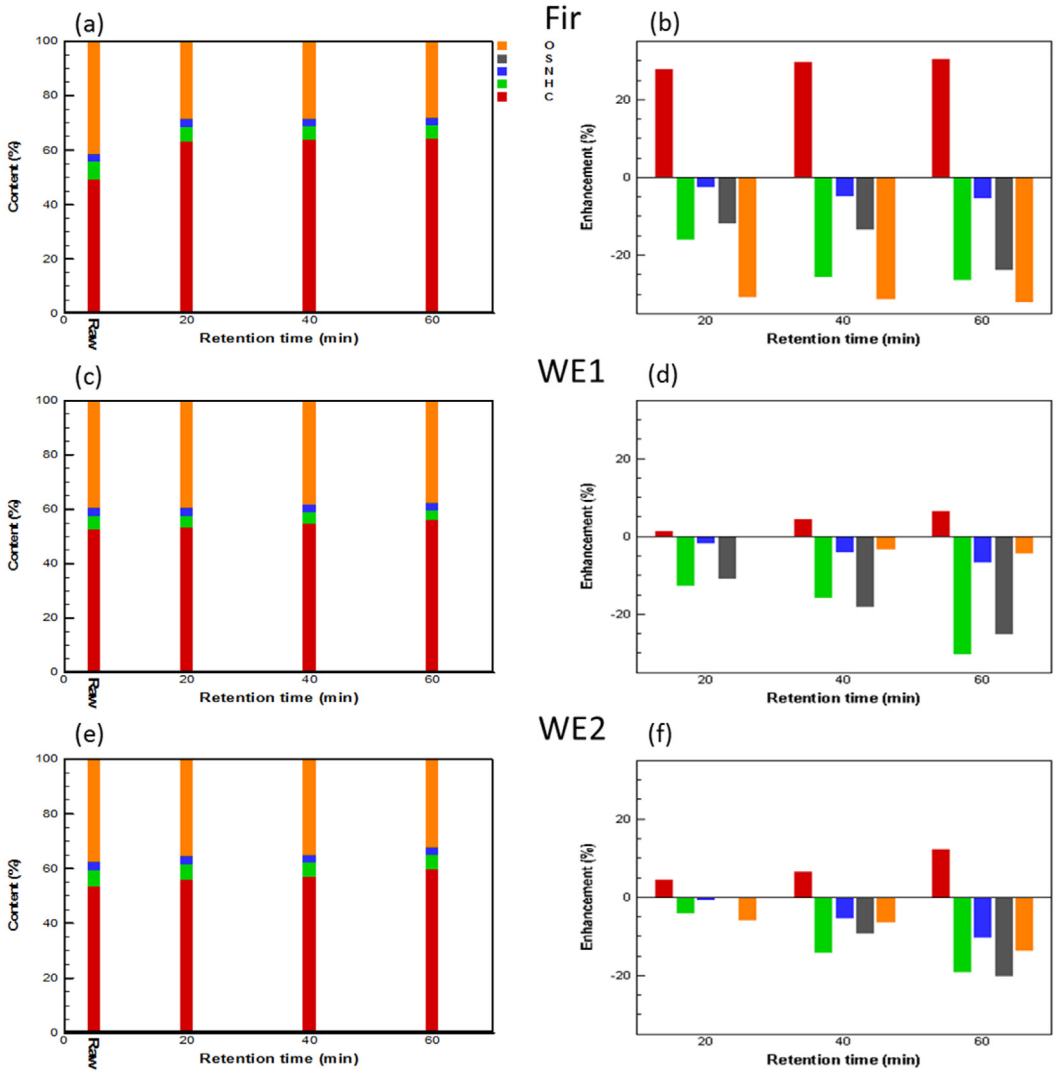

Fig. 5. The elemental analysis of torrefied biomass from three pure materials.

lowest HHV (17.9 MJ/kg) among all the materials, it recorded the highest HHV (averagely 25.8 MJ/kg) after torrefaction treatment (22.8 MJ/kg for WE1 and 25.5 MJ/kg for WE2 in average). Hydrogen and oxygen contents also diminished to a greater extent for fir compared to waste epoxy resins. That would further intensify the energy density and provide the highest enhancement of HHV for the fir. Nitrogen and sulfur contents were also reduced after torrefaction. This was beneficial to the environment since NOx and SOx might be emitted during combustion in the biofuel (Jafarinejad, 2016; Shimokuri et al., 2015), respectively.

Both H/C and O/C ratios shown in Fig. 6 descended after torrefaction, which rendered the products to be closer to the properties of coal (Chen et al., 2012). The average of H/C ratio dropped from 1.56 to 0.93, 1.11 to 0.86, and 1.38 to 1.13 for fir, WE1, and WE2, respectively, revealing that the effect of torrefaction was more conspicuous on fir than on waste epoxy resins. The same trend was also observed in the O/C ratio. While the O/C ratio went down for almost half for fir, the reduction extents of the two waste epoxy resins were within 10% only. For the effect of duration on the two ratios, the ANOVA test suggested that the effect was statistically significant on the H/C ratio (p-value <0.05) but not on the O/C ratio (p-value>0.05). From the elemental analysis (Fig. 5), the variation of carbon and oxygen contents of fir was not large by increasing the duration, but it was significant for hydrogen (Fig. 5b, d, and **f**). From the ANOVA test, the difference between the fir and waste epoxy resins was also greatly significant (p-value < 0.005) for both the H/C and O/C ratios.

3.4.2. Mixtures

The theoretical and experimental values of the H/C and O/C ratios were plotted in Fig. 7. It revealed an antagonistic effect on all the O/C ratios, regardless of WE1, WE2, and different mixing ratios. From the result of the one-tail student

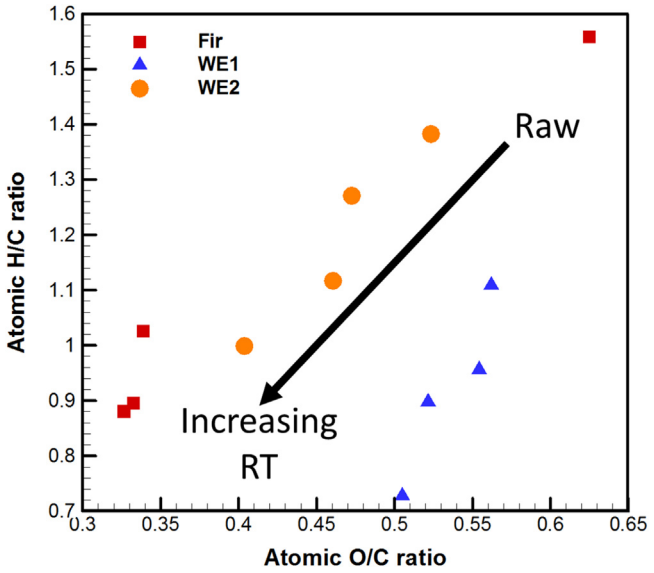

Fig. 6. Atomic H/C and O/C ratios of three pure materials undergoing torrefaction treatment with different retention time (RT).

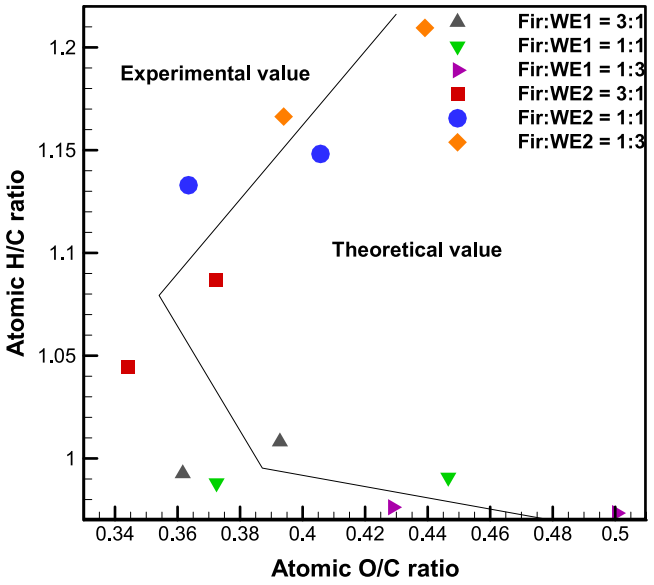

Fig. 7. Theoretical and experimental values of atomic H/C and O/C ratios for the six mixtures with different blending ratios.

t-test, the difference between the theoretical and experimental value was statistically significant (p-value < 0.05) in terms of the O/C ratio. While all the carbon contents presented a synergistic effect, irrespective of mixing ratio and materials, all the oxygen contents showed an antagonistic effect (results not shown). Thus, the important difference between theoretical and experimental O/C ratio could be well-explained.

On the other hand, the difference of the H/C ratio between theoretical and experimental value was statistically significant for the mixtures of WE2 and fir (p-value < 0.05) but not for WE1 and fir (p-value > 0.05). When looking into the SE for carbon and hydrogen contents, the extent for carbon (mean 4.02%) and hydrogen (mean 2.84%) contents are similar for WE1 and fir mixtures. On the contrary, WE2 and fir mixtures displayed a huge difference between the SE for carbon (mean 3.06%) and for hydrogen (mean 0.0029%). As a result, the significance of SE for the H/C ratio had the opposite performance in the two mixtures due to the different thermal resistance for WE1 and WE2.

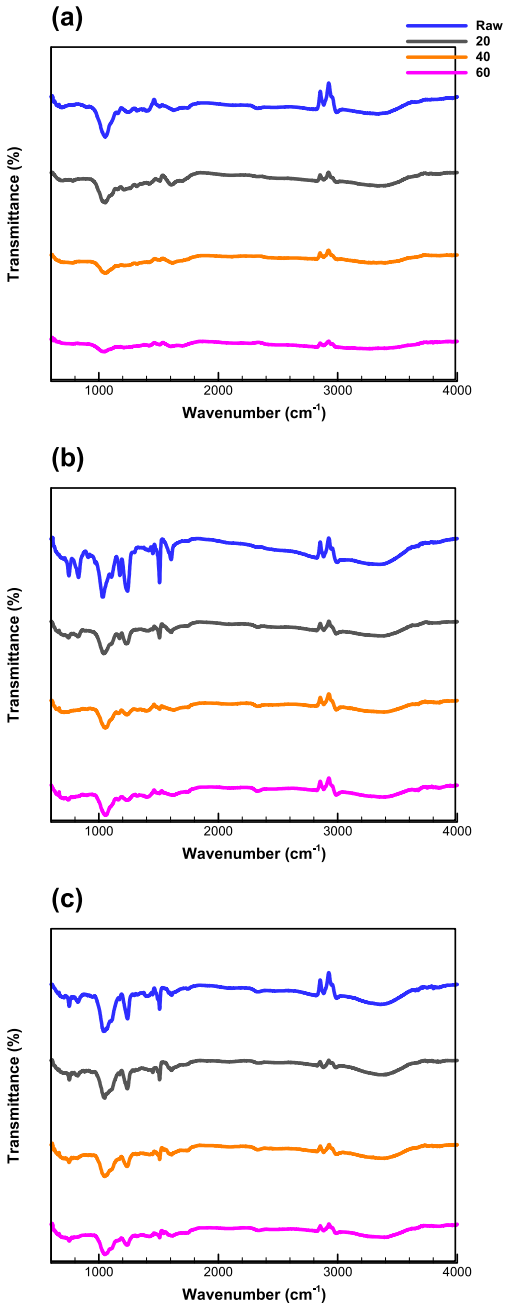

Fig. 8. FTIR spectra of raw and torrefied (a) fir, (b) WE1, and (c) WE2 with different torrefaction durations.

3.5. FTIR spectrum

The FTIR spectra of fir in Fig. 8a showed that most of the chemical bonding was diminished after torrefaction treatment. The peaks during 1020–1150 cm^{-1} represented the C–O bonds for alcohol. During torrefaction, they gradually decreased together with other volatile matters (Farooq et al., 2018). Other chemical bonds such as phenolic compounds (1160–1270 cm^{-1}), C–H bond for alkanes (1350–1480 cm^{-1}), aromatic rings (1460–1510 cm^{-1}), C=C bond for alkenes (1620–1680 cm^{-1}), C=O for carbonyl groups (1650–1800 cm^{-1}), C–H bond for alkanes (2850–3000 cm^{-1}), and O–H bond for alcohols and phenols (3200–3600 cm^{-1}) (**Table S1**) shown in raw fir were all decreased with increasing retention time.

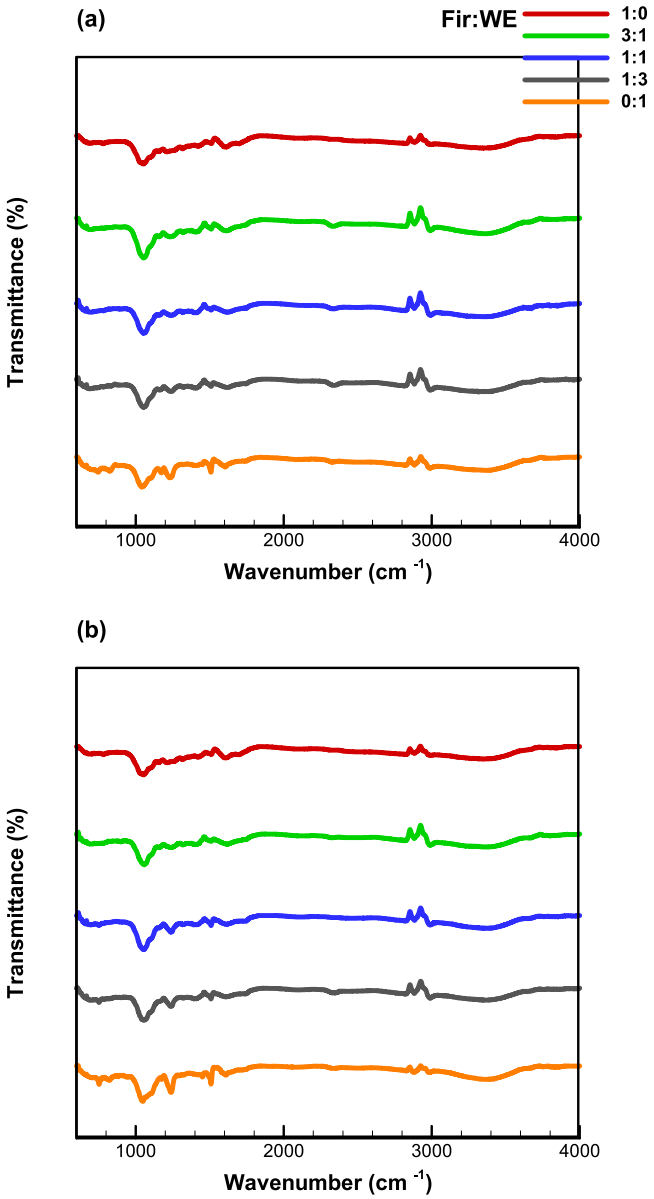

Fig. 9. FTIR spectra of the mixtures of (a) fir and WE1 and (b) fir and WE2 at different mixing ratios.

The chemical bonding in WE1 and WE2 were very similar in that the peaks built on almost the same wavenumbers in the spectra in Fig. 8b and c. However, several chemicals were more significant such as the C–Cl, phenolic compounds, aromatic rings, and O–H bonds for WE1. Sodium chloride is one of the major catalysts used in the production of epoxy resin and thus will usually be present in the intermediates (Chen et al., 2020b). In addition, since WE1 is a phenolic epoxy resin, there should be more phenolic compounds and O–H bonds in WE1 than WE2, as shown in Fig. 8. Furthermore, as mentioned earlier, WE1 possessed higher heat resistance property because of its cross-linked aromatic rings. This was proven by the FTIR results which shown higher aromatic ring contents compared to WE2. The performance of waste epoxy resin with varying durations was similar to fir. All the chemical bonds were gradually diminished with increasing duration. The torrefaction demonstrated a higher impact on fir rather than on WE1 or WE2. Consequently, there are many other peaks remained in the FTIR spectra for torrefied waste epoxy resin but not for fir, even after 60-min torrefaction.

The FTIR spectra of 20-min torrefied mixtures were exhibited in Fig. 9. The SE for each wavenumber was conducted but all of the values were lower than 2.2%. The difference between theoretical and experimental was not statistically significant as judged by the t-test as well. Therefore, the theoretical lines were not reported here. Generally, all the peaks were in the right tendency. In other words, the values were logically laid between fir and intermediate waste epoxy

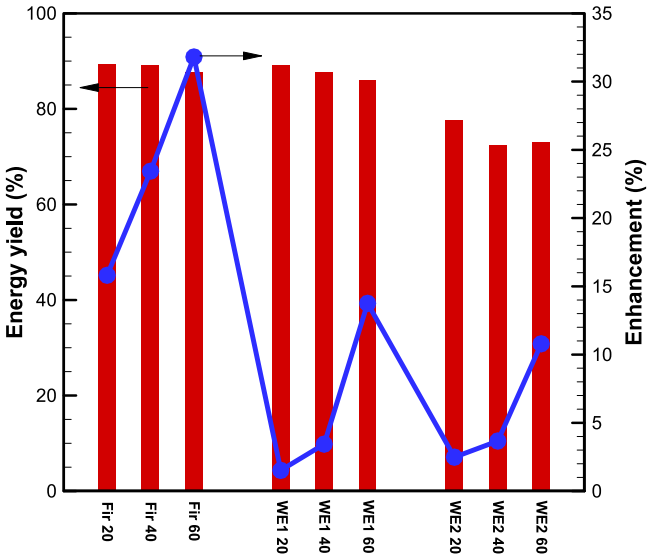

Fig. 10. Profiles of total energy yield 1 and its enhancement of biochar and liquid products from three individual materials through torrefaction with three different retention times. (bar: energy yield (%), and line: enhancement (%)).

resins. The other important observation was that co-torrefaction could render the quality of the products to be more homogeneous. Irrespective of materials and mixing ratios, the six mixtures presented here exhibited very similar FTIR spectra, regardless of the quality or quantity. That would benefit the product application as biofuels since it would be very hard to control the combustion parameters if the properties of fuels were not uniform.

3.6. Bio-oil

3.6.1. Energy yield—liquid product

Even though the main product after torrefaction was biochar, the bio-oil was also an added-value product since it could be used for energy application. The total energy yield, including biochar and bio-oil, was calculated as follows

$$\text{Total energy yield 1} = \frac{\text{HHV of biochar} \times \text{solid yield} + \text{HHV of bio-oil} \times \text{liquid yield}}{\text{HHV of raw material}} \tag{3}$$

The profiles of the total energy yield and the enhancement of bio-oil were shown in Fig. 10. The HHV of bio-oil was analyzed after homogenized the liquid product and sampled through the middle point. It demonstrated that the energy yield was improved, especially for fir where the improvement was between 15.8 and 31.8%. Due to the lower heat resistance, most of the structure inside the fir was disintegrate and became liquid products (Chen et al., 2020a). If these liquid products could be upgraded for energy application, the energy yield of fir would be the highest. The enhancement values of waste epoxy resins were relatively lower since most of the energy remained in the solid product due to their high heat resistance. All the enhancement values ascended with increasing duration. That was due to the longer time for feedstock to receive heat which led to more energy loss following the liberated volatile matters (Bach et al., 2017). **Fig. S1a** illustrated that the color of liquid products became darker with increasing duration due to the deposition of more compounds with higher heating value. The color of the liquid product from fir was the darkest, so its heating value was superior to those of the waste epoxy resins. This led to the highest improvement for fir on total energy yield after torrefaction. In order to analyze the bio-oil in detail, Fir 20, Fir 40, Fir 60, WE1 60, and WE2 60 were chosen for further analysis due to their significant improvement (>10% enhancement).

3.6.2. Energy yield—oil and tar

The liquid products from torrefaction could be divided into two parts, namely, oil and tar. To enable the separation of the oil from tar, these liquid products were kept stationary on the rack for over three days (**Fig. S1b**). Thereafter, it was observed that the tar was separated from the oil to form two phases as all the tar had sedimented. Both the tar and oil were weighed and their HHVs were measured separately with pipettes. Thereafter, the liquid yield could be further partitioned into oil and tar yields which were depicted in Fig. 11, as well as their corresponding HHVs.

Both oil and tar yields were found to be the lowest for WE1 because of its highest intrinsic heat resistance characteristic. For fir, the total amount of liquid product was quite consistent within the three durations. However, a longer duration would naturally result in more heavy contents (tar) transforming into light contents (oil). Consequently, the oil yield gradually increased while the tar yield decreased with ascending duration. The HHVs of produced tars (Fig. 11b) were

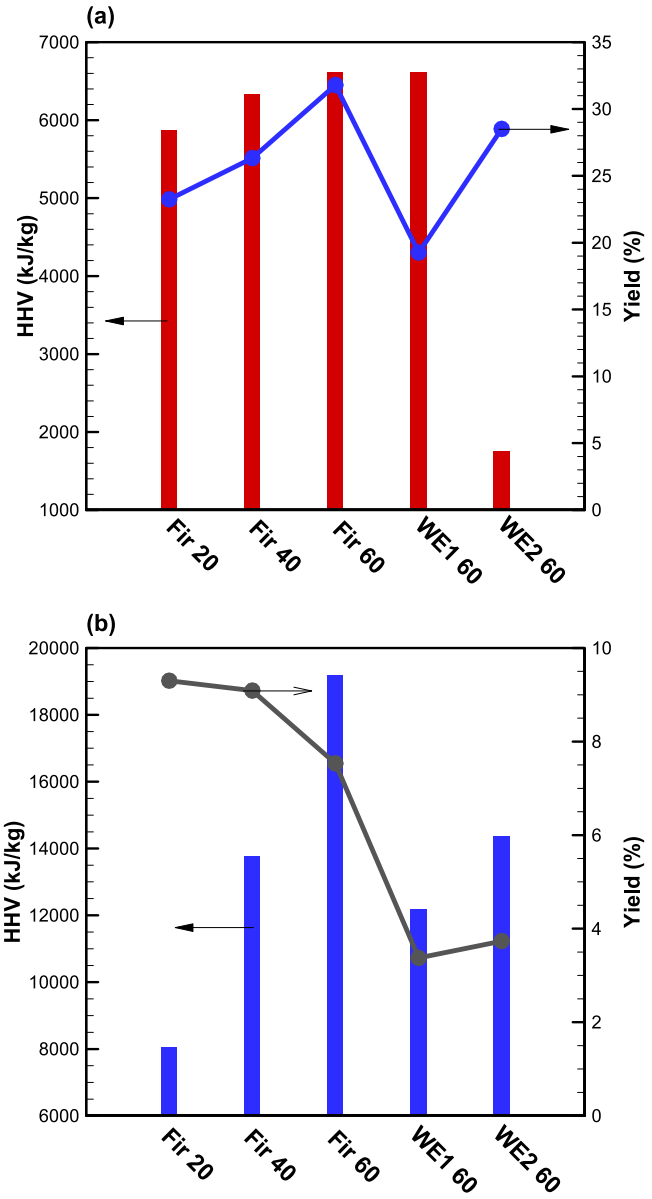

Fig. 11. Profiles of HHV and yield of (a) oil and (b) tar. (bar: HHV (kJ/kg), and line: Yield (%)).

higher than those of the oils (Fig. 11a). Most of the tars contained heavier compounds with high energy density compared to the liquid oils. Moreover, the water content would mainly be retained in the oil phase and thereby reduced its HHV (Chen et al., 2015b). The water content in oil produced from WE2 (∼90%) was greater than from WE1 (∼70%) judged by ASTM D4928. This could be explained by the higher moisture content in WE2 than in WE1, as seen in Fig. 3.

Based on the data in Fig. 11, a new total energy yield formula was developed as presented below:

$$\text{Total energy yield 2} = \frac{\text{HHV of biochar} \times \text{solid yield} + \text{HHV of oil} \times \text{oil yield} + \text{HHV of tar} \times \text{tar yield}}{\text{HHV of raw material}} \quad (4)$$

Unfortunately, all the enhancement rates decreased albeit the calculation was closer to the real situation (Fig. 12). The enhancement diminished by approximately 0.5, 0.9, 2, 4.5, and 7.1% for Fir 20, Fir 40, Fir 60, WE1 60, and WE2 60, respectively. This was due to the overestimation by Eq. (3) of the total energy yield. The HHV of the liquid product from Eq. (3) was determined after homogenized the liquid sample. Using the mixed solution to represent the overall HHV might not be accurate since tars would exist in the whole liquid space after homogenized. The results clearly showed that tar was the main energy source (Fig. 11b) for the liquid product, although the yield was dominated by the liquid oil. As a result, most of the liquids were oil with lower HHV. Furthermore, it could be concluded that the two equations would be

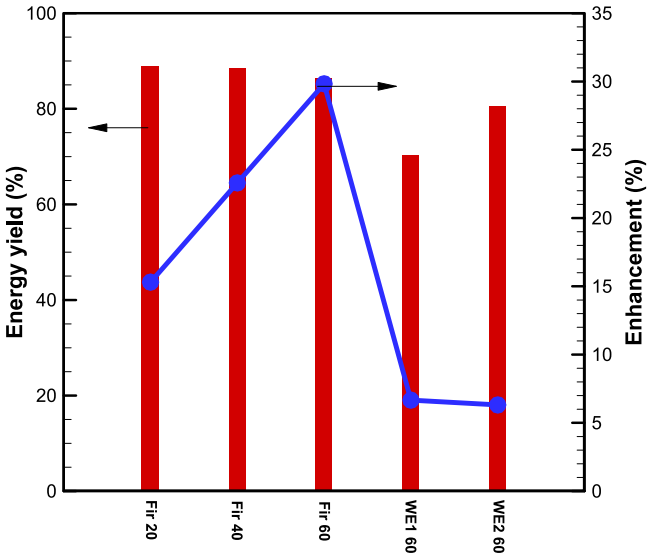

Fig. 12. The total energy yield 2 and its enhancement of biochar + oil + tar under the torrefaction temperature of 300 °C. (bar: energy yield (%), and line: Enhancement (%)).

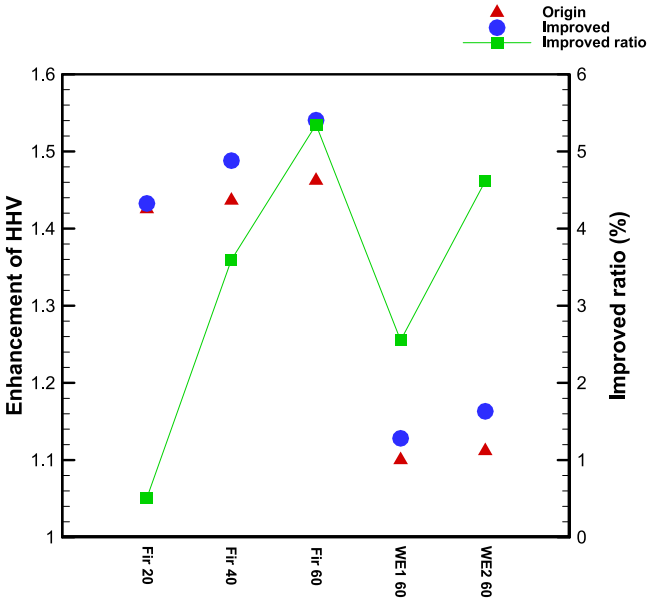

Fig. 13. The enhancement of HHV of the biochar after tar improvement.

almost equal if the tar yield was high or the HHV for oil and tar were similar to each other. These would reduce the total energy yield disparity before and after quiescence.

3.6.3. Improved biochar

Although tar was regarded as the main energy source in the liquid product, many experimental studies in the literature treated it as an unwanted byproduct of torrefaction (Fan et al., 2020; Huang et al., 2019). Tar was easier to choke the facilities or pipes (Prins et al., 2006). That was attributed to its high viscosity since it contained a lot of heavy chemicals. On the contrary, oil did not possess high HHV but it was relatively more convenient to be used in real applications with less viscosity (Chih et al., 2020; Mwangi et al., 2014). Nonetheless, it was a pity to discard tar as a waste since it had inherently higher HHV compared to oil.

In view of the sustainability and circular economy concept, a method had been devised to reuse tar to coat onto biochar which could further improve the biochar's HHV. Due to the amount limitation, 0.5 mL tar controlled by pipette was added

into a corresponding 0.5 g biochar. After evenly stirring, the improved biochar was put in the oven at a temperature of 105 °C for at least 12 h, so the dry basis would be the same as raw biochar for HHV measurement. From the FTIR spectra in **Fig. S2**, the tar was successfully coated onto the biochar as the improved biochar had several distinctive peaks which were only shown in the tar spectrum. Fig. 13 displayed the enhancement of HHV before and after the tar improvement. It was very obvious that the effect of the tar coating was pronounced. The t-test also confirmed that the improvement was statistically significant (p-value < 0.05). The order of improved ratio was Fir 60 > WE2 60 > Fir 40 > WE1 60 > Fir 20 and that was the same as the order of HHV of tar. The coating process should be uniform for all the samples so that these two orders were the same. Furthermore, the porosity of biochar was larger than the raw biomass, which benefited the adsorption of tar (Chen et al., 2012). As a whole, the method of reusing tar for the HHV improvement of biochar was a feasible method which not only removed the unwanted byproduct but also treated it as a useful additive and synchronized with the waste-to-energy vision.

4. Conclusions

Co-torrefaction of fir and two kinds of intermediate waste epoxy resins were investigated by a batch type reactor. Both the synergistic and antagonistic effects were discovered during the experiments. Generally, the catalyst impact caused by the sodium content in the waste epoxy resins would be dominant when the retention time was short and increased the volatile matter liberation. On the other hand, the blocking effect would take over in the case of longer retention time. For elemental analysis, all the carbon content presented a synergistic phenomenon while the oxygen content displayed an antagonistic effect irrespective of the materials. That resulted in a great antagonistic effect in the O/C ratio. The interaction reaction between fir and intermediate waste epoxy resins for the H/C ratio was not necessarily depending on WE1 or WE2. Overall, a short duration was more promising in terms of energy yield. Furthermore, the energy yield could be further improved if the liquid product from the torrefaction process was separated and recycled properly for biochar burning.

CRediT authorship contribution statement

Chia-Yang Chen: Data collection, Methodology, Validation, Investigation, Writing - original draft. **Wei-Hsin Chen:** Conceptualization, Formal analysis, Funding acquisition, Investigation, Project administration, Resources, Supervision, Writing - review & editing. **Steven Lim:** Investigation, Writing - review & editing. **Hwai Chyuan Ong:** Investigation, Writing - review & editing. **Aristotle T. Ubando:** Investigation Writing - review & editing.

Declaration of competing interest

The authors declare that they have no known competing financial interests or personal relationships that could have appeared to influence the work reported in this paper.

Acknowledgments

The authors acknowledge the financial support and materials provided by Nan Ya Plastics Corporation for this research, and fir samples provided by CPC Corporation, Taiwan. The authors also gratefully acknowledge the financial support of the Ministry of Science and Technology , Taiwan, R.O.C., under the grant numbers MOST 109-2221-E-006-040-MY3 and MOST 109-3116-F-006-016-CC1 for this research.

Appendix A. Supplementary data

Supplementary material related to this article can be found online at https://doi.org/10.1016/j.eti.2020.101218.

References

Babinszki, B., Jakab, E., Sebestyén, Z., Blazsó, M., Berényi, B., Kumar, J., Krishna, B.B., Bhaskar, T., Czégény, Z., 2020. Comparison of hydrothermal carbonization and torrefaction of azolla biomass: Analysis of the solid products. J. Anal. Appl. Pyrolysis 104844.

Bach, Q.-V., Chen, W.-H., Lin, S.-C., Sheen, H.-K., Chang, J.-S., 2017. Wet torrefaction of microalga Chlorella vulgaris ESP-31 with microwave-assisted heating. Energy Convers. Manage. 141, 163–170.

Brebu, M., Ucar, S., Vasile, C., Yanik, J., 2010. Co-pyrolysis of pine cone with synthetic polymers. Fuel 89 (8), 1911–1918.

Chang, Y.-H., Chen, W., Chang, N.-B., 1998. Comparative evaluation of RDF and MSW incineration. J. Hazard. Mater. 58 (1–3), 33–45.

Chen, C.-Y., Chen, W.-H., 2020. Co-torrefaction followed by co-combustion of intermediate waste epoxy resins and woody biomass in the form of mini-pellet. Int. J. Energy Res. 1–16.

Chen, C.-Y., Chen, W.-H., Hung, C.-H., 2021. Combustion performance and emissions from torrefied and water washed biomass using a kg-scale burner. J. Hard Mater. 402, 123468.

Chen, C.-Y., Chen, W.-H., Ilham, Z., 2020a. Effects of torrefaction and water washing on the properties and combustion reactivity of various wastes. Int. J. Energy Res. 1–15.

Chen, X., Hou, J., Gu, Q., Wang, Q., Gao, J., Sun, J., Fang, Q., 2020b. A non-bisphenol-A epoxy resin with high Tg derived from the bio-based protocatechuic acid: Synthesis and properties. Polymer 122443.

Chen, W.-H., Huang, M.-Y., Chang, J.-S., Chen, C.-Y., Lee, W.-J., 2015a. An energy analysis of torrefaction for upgrading microalga residue as a solid fuel. Bioresour. Technol. 185, 285–293.
Chen, C.-Y., Lee, W.-J., Mwangi, J.K., Wang, L.-C., Wu, J.-L., Lin, S.-L., 2017a. Reduction of persistent organic pollutant emissions during incinerator start-up by using crude waste cooking oil as an alternative fuel. Aerosol Air Qual. Res. 17, 899–912.
Chen, C.-Y., Lee, W.-J., Wang, L.-C., Chang, Y.-C., Yang, H.-H., Young, L.-H., Lu, J.-H., Tsai, Y.I., Cheng, M.-T., Mwangi, J.K., 2017b. Impact of high soot-loaded and regenerated diesel particulate filters on the emissions of persistent organic pollutants from a diesel engine fueled with waste cooking oil-based biodiesel. Appl. Energy 191, 35–43.
Chen, W.-H., Lin, B.-J., Colin, B., Chang, J.-S., Pétrissans, A., Bi, X., Pétrissans, M., 2018. Hygroscopic transformation of woody biomass torrefaction for carbon storage. Appl. Energy 231, 768–776.
Chen, W.-H., Liu, S.-H., Juang, T.-T., Tsai, C.-M., Zhuang, Y.-Q., 2015b. Characterization of solid and liquid products from bamboo torrefaction. Appl. Energy 160, 829–835.
Chen, W.-H., Lu, K.-M., Lee, W.-J., Liu, S.-H., Lin, T.-C., 2014. Non-oxidative and oxidative torrefaction characterization and SEM observations of fibrous and ligneous biomass. Appl. Energy 114, 104–113.
Chen, W.-H., Lu, K.-M., Tsai, C.-M., 2012. An experimental analysis on property and structure variations of agricultural wastes undergoing torrefaction. Appl. Energy 100, 318–325.
Chen, W.-H., Peng, J., Bi, X.T., 2015c. A state-of-the-art review of biomass torrefaction, densification and applications. Renew. Sustain. Energy Rev. 44, 847–866.
Cheruiyot, N.K., Hou, W.-C., Wang, L.-C., Chen, C.-Y., 2019. The impact of low to high waste cooking oil-based biodiesel blends on toxic organic pollutant emissions from heavy-duty diesel engines. Chemosphere 235, 726–733.
Chih, Y.-K., Chen, W.-H., Tran, K.-Q.J.F., 2020. Hydrogen production from methanol partial oxidation through the catalyst prepared using torrefaction liquid products. 279, 118419.
Chikhi, N., Fellahi, S., Bakar, M., 2002. Modification of epoxy resin using reactive liquid (ATBN) rubber. Eur. Polym. J. 38 (2), 251–264.
Correia, R., Gonçalves, M., Nobre, C., Mendes, B., 2017. Impact of torrefaction and low-temperature carbonization on the properties of biomass wastes from Arundo donax L. and Phoenix canariensis. Bioresour. Technol. 223, 210–218.
Cui, J., Forssberg, E., 2003. Mechanical recycling of waste electric and electronic equipment: a review. J. Hazard. Mater. 99 (3), 243–263.
Cui, J.-l., Luo, C.-l., Tang, C.W.-y., Chan, T.-s., Li, X.-d., 2017. Speciation and leaching of trace metal contaminants from e-waste contaminated soils. J. Hard Mater. 329, 150–158.
Darmstadt, H., Garcia-Perez, M., Chaala, A., Cao, N.-Z., Roy, C., 2001. Co-pyrolysis under vacuum of sugar cane bagasse and petroleum residue: Properties of the char and activated char products. Carbon 39 (6), 815–825.
Fan, Y., Tippayawong, N., Wei, G., Huang, Z., Zhao, K., Jiang, L., Zheng, A., Zhao, Z., Li, H., 2020. Minimizing tar formation whilst enhancing syngas production by integrating biomass torrefaction pretreatment with chemical looping gasification. Appl. Energy 260, 114315.
Farooq, M.Z., Zeeshan, M., Iqbal, S., Ahmed, N., Shah, S.A.Y., 2018. Influence of waste tire addition on wheat straw pyrolysis yield and oil quality. Energy 144, 200–206.
Ge, S., Foong, S.Y., Ma, N.L., Liew, R.K., Mahari, W.A.W., Xia, C., Yek, P.N.Y., Peng, W., Nam, W.L., Lim, X.Y., 2020. Vacuum pyrolysis incorporating microwave heating and base mixture modification: An integrated approach to transform biowaste into eco-friendly bioenergy products. Renew. Sustain. Energy Rev. 127, 109871.
Gil, M.V., García, R., Pevida, C., Rubiera, F., 2015. Grindability and combustion behavior of coal and torrefied biomass blends. Bioresour. Technol. 191, 205–212.
Huang, C.-L., Bao, L.-J., Luo, P., Wang, Z.-Y., Li, S.-M., Zeng, E.Y., 2016. Potential health risk for residents around a typical e-waste recycling zone via inhalation of size-fractionated particle-bound heavy metals. J. Hard Mater. 317, 449–456.
Huang, J., Qiao, Y., Wei, X., Zhou, J., Yu, Y., Xu, M., 2019. Effect of torrefaction on steam gasification of starchy food waste. Fuel 253, 1556–1564.
Jafarinejad, S., 2016. Control and treatment of sulfur compounds specially sulfur oxides (SOx) emissions from the petroleum industry: a review. Chem. Int. 2 (4), 242–253.
John Kennedy, M., Wen-Jhy, L.E.E., Lin-Chi, W., Nicholas Kiprotich, C., Chia-Yang, C., Farran, R., 2015. An overview: Emission of brominated persistent organic compounds in the diesel engine exhaust. エアロゾル研究 30 (4), 254–260.
Keivani, B., Gultekin, S., Olgun, H., Atimtay, A.T., 2018. Torrefaction of pine wood in a continuous system and optimization of torrefaction conditions. Int. J. Energy Res. 42 (15), 4597–4609.
Khazraie Shoulaifar, T., DeMartini, N., Karlström, O., Hupa, M., 2016. Impact of organically bonded potassium on torrefaction: Part 1. Experimental. Fuel 165, 544–552.
Kim, Y.-H., Lee, S.-M., Lee, H.-W., Lee, J.-W., 2012. Physical and chemical characteristics of products from the torrefaction of yellow poplar (Liriodendron tulipifera). Bioresour. Technol. 116, 120–125.
Kutlu, O., Kocar, G., 2018. Upgrading lignocellulosic waste to fuel by torrefaction: Characterisation and process optimization by response surface methodology. Int. J. Energy Res. 42 (15), 4746–4760.
Labunska, I., Abdallah, M.A.-E., Eulaers, I., Covaci, A., Tao, F., Wang, M., Santillo, D., Johnston, P., Harrad, S., 2015. Human dietary intake of organohalogen contaminants at e-waste recycling sites in Eastern China. Environ. Int. 74, 209–220.
Lam, S.S., Mahari, W.A.W., Ok, Y.S., Peng, W., Chong, C.T., Ma, N.L., Chase, H.A., Liew, Z., Yusup, S., Kwon, E.E., 2019. Microwave vacuum pyrolysis of waste plastic and used cooking oil for simultaneous waste reduction and sustainable energy conversion: Recovery of cleaner liquid fuel and techno-economic analysis. Renew. Sustain. Energy Rev. 115, 109359.
Lu, J.-J., Chen, W.-H., 2013. Product yields and characteristics of corncob waste under various torrefaction atmospheres. Energies 7 (1), 13–27.
Lu, K.-M., Lee, W.-J., Chen, W.-H., Lin, T.-C., 2013. Thermogravimetric analysis and kinetics of co-pyrolysis of raw/torrefied wood and coal blends. Appl. Energy 105, 57–65.
Mazaheri, H., Lee, K.T., Mohamed, A.R., 2013. Influence of temperature on liquid products yield of oil palm shell via subcritical water liquefaction in the presence of alkali catalyst. Fuel Process. Technol. 110, 197–205.
Mwangi, J.K., Lee, W.-J., Whang, L.-M., Wu, T.S., Chen, W.-H., Chang, J.-S., Chen, C.-Y., Chen, C.-L.J.A., research, a.q., 2014. Microalgae oil: Algae cultivation and harvest, algae residue torrefaction and diesel engine emissions tests. 15(1) 81-98.
Ong, H.C., Chen, W.-H., Singh, Y., Gan, Y.Y., Chen, C.-Y., Show, P.L., 2020. A state-of-the-art review on thermochemical conversion of biomass for biofuel production: A TG-FTIR approach. Energy Convers. Manage. 209, 112634.
Pimchuai, A., Dutta, A., Basu, P., 2010. Torrefaction of agriculture residue to enhance combustible properties. Energy Fuels 24 (9), 4638–4645.
Prins, M.J., Ptasinski, K.J., Janssen, F.J.J.G., 2006. More efficient biomass gasification via torrefaction. Energy 31 (15), 3458–3470.
Sadaka, S., Negi, S., 2009. Improvements of biomass physical and thermochemical characteristics via torrefaction process. Environ. Prog. Sustain. Energy 28 (3), 427–434.
Sajdak, M., 2017. Impact of plastic blends on the product yield from co-pyrolysis of lignin-rich materials. J. Anal. Appl. Pyrolysis 124, 415–425.
Sher, F., Iqbal, S.Z., Liu, H., Imran, M., Snape, C.E., 2020. Thermal and kinetic analysis of diverse biomass fuels under different reaction environment: A way forward to renewable energy sources. Energy Convers. Manage. 203, 112266.

Shimokuri, D., Fukuba, S., Ishizuka, S., 2015. Fundamental investigation on the fuel-NOx emission of the oxy-fuel combustion with a tubular flame burner. Proc. Combust. Inst. 35 (3), 3573–3580.
van der Stelt, M.J.C., Gerhauser, H., Kiel, J.H.A., Ptasinski, K.J., 2011. Biomass upgrading by torrefaction for the production of biofuels: A review. Biomass Bioenergy 35 (9), 3748–3762.
Tsai, J.-H., Lin, S.-L., Mwangi, J.K., Chen, C.-Y., Wu, T.S., 2015. Energy saving and pollution reduction by adding water containing iso-butanol and iso-propyl alcohol in a diesel engine. Aerosol Air Qual. Res. 15, 2115–2128.
Wu, W., Qiu, K., 2014. Vacuum co-pyrolysis of chinese fir sawdust and waste printed circuit boards. Part I: Influence of mass ratio of reactants. J. Anal. Appl. Pyrolysis 105, 252–261.
Yang, F., Sun, C., Huang, G., 2018. Study on cross-strait energy cooperation under the new circumstance. J. Cleaner Prod. 180, 97–106.
Yang, N., Zhang, H., Chen, M., Shao, L.-M., He, P.-J., 2012. Greenhouse gas emissions from MSW incineration in China: Impacts of waste characteristics and energy recovery. Waste Manage. 32 (12), 2552–2560.
Yao, L., Shi, X., Andrews-Speed, P., 2018. Conceptualization of energy security in resource-poor economies: The role of the nature of economy. Energy Policy 114, 394–402.
Zhao, G.-h., Luo, X.-z., Qiao, J., Chen, G., 2017. Investigation of the leaching characteristics of heavy metals from waste printed circuit boards through column testing with simulated acid rain. J. Residuals Sci. Technol..